RESEARCH ARTICLE | *Cellular and Molecular Properties of Neurons*

Glycolytic inhibition by 2-deoxy-D-glucose abolishes both neuronal and network bursts in an in vitro seizure model

Li-Rong Shao and Carl E. Stafstrom

Division of Pediatric Neurology, Department of Neurology, Johns Hopkins University School of Medicine, Baltimore, Maryland

Shao LR, Stafstrom CE. Glycolytic inhibition by 2-deoxy-D-glucose abolishes both neuronal and network bursts in an in vitro seizure model. *J Neurophysiol* 118: 103–113, 2017. First published April 12, 2017; doi:10.1152/jn.00100.2017.—Neuronal activity is energy demanding and coupled to cellular metabolism. In this study, we investigated the effects of glycolytic inhibition with 2-deoxy-D-glucose (2-DG) on basal membrane properties, spontaneous neuronal firing, and epileptiform network bursts in hippocampal slices. The effect of glycolytic inhibition on basal membrane properties was examined in hippocampal CA1 neurons, which are not ordinarily active spontaneously. Intracellular application of 2-DG did not significantly alter the membrane input resistance, action-potential threshold, firing pattern, or input-output relationship of these neurons compared with simultaneously recorded neighboring neurons without intracellular 2-DG. The effect of glycolytic inhibition on neuronal firing was tested in spontaneously active hippocampal neurons (CA3) when synaptic transmission was left intact or blocked with AMPA, NMDA, and GABA$_A$ receptor antagonists (DNQX, APV, and bicuculline, respectively). Under both conditions (synaptic activity intact or blocked), bath application of 2-DG (2 mM) blocked spontaneous firing in ~2/3 (67 and 71%, respectively) of CA3 pyramidal neurons. In contrast, neuronal firing of CA3 neurons persisted when 2-DG was applied intracellularly, suggesting that glycolytic inhibition of individual neurons is not sufficient to stop neuronal firing. The effects of 2-DG on epileptiform network bursts in area CA3 were tested in Mg^{2+}-free medium containing 50 μM 4-aminopyridine. Bath application of 2-DG abolished these epileptiform bursts in a dose-dependent and all-or-none manner. Taken together, these data suggest that altered glucose metabolism profoundly affects cellular and network hyperexcitability and that glycolytic inhibition by 2-DG can effectively abrogate epileptiform activity.

NEW & NOTEWORTHY Neuronal activity is highly energy demanding and coupled to cellular metabolism. In this study, we demonstrate that glycolytic inhibition with 2-deoxy-D-glucose (2-DG) effectively suppresses spontaneous neuronal firing and epileptiform bursts in hippocampal slices. These data suggest that an altered metabolic state can profoundly affect cellular and network excitability, and that the glycolytic inhibitor 2-DG may hold promise as a novel treatment of drug-resistant epilepsy.

glucose metabolism; hippocampus; epilepsy; cellular excitability; patch clamp

Address for reprint requests and other correspondence: L.-R. Shao, Div. of Pediatric Neurology, Dept. of Neurology, Johns Hopkins Univ. School of Medicine, 200 N. Wolfe St., Baltimore, MD 21287 (e-mail: lshao5 @jhmi.edu).

BRAIN ACTIVITY is highly demanding energetically and is tightly coupled to its metabolic state as demonstrated by functional brain imaging (Magistretti and Pellerin 1996; Raichle and Mintun 2006). During pathologically hyperactive states such as seizures, the brain's energy demand is even higher. Because the brain utilizes glucose as its obligate energy source, glucose metabolism plays a central role in maintaining seizure activity (Hertz and Dienel 2002). Indeed, limiting glucose intake (i.e., fasting; Conklin 1922; Geyelin 1921) or switching from glucose to ketone bodies (i.e., ketogenic diet) has proven to be highly effective in controlling seizures in patients with medically refractory epilepsy (Freeman and Vining 1998; Huttenlocher 1976; Stafstrom and Rho 2012; Thakur et al. 2014) and in experimental models (Kim et al. 2015; Lutas and Yellen 2013). Thus altering energy metabolism may represent a novel strategy and alternative therapy for seizure control, particularly for those resistant to drugs (Kawamura et al. 2016). We and others previously proposed that direct inhibition of glycolysis leads to seizure control and that the glycolytic inhibitor 2-deoxy-D-glucose (2-DG) produces acute anticonvulsant effects in vitro (Forte et al. 2016; Stafstrom et al. 2009) and chronic antiepileptic effects in vivo (Garriga-Canut et al. 2006; Gasior et al. 2010; Stafstrom et al. 2009). Specifically, we previously showed that 2-DG decreases epileptiform activity induced by elevated extracellular potassium, 4-aminopyridine (4-AP), and bicuculline in brain slices from adult animals (Stafstrom et al. 2009). Chronic antiepileptic actions of 2-DG have been demonstrated in rats kindled from the perforant path or olfactory bulb (Garriga-Canut et al. 2006; Stafstrom et al. 2009). However, the mechanism by which 2-DG alters cellular and network excitability and the full spectrum of its effects are not yet known (Stafstrom and Sutula 2017). 2-DG is a glucose analog with one oxygen atom removed at the 2-position. 2-DG is taken up into cells by glucose transporters, after which it is phosphorylated to 2-deoxy-glucose 6-phosphate (2-DG-6P), which cannot be further metabolized, thus inhibiting glycolysis by limiting the production of fructose-6-phosphate (F-6-P) from G-6-P (Fig. 1) (Sokoloff et al. 1977).

In this study, we aimed to further understand how altered glucose metabolism can affect cellular and network excitability by addressing the following questions: *1*) Does glycolytic inhibition alter basal intrinsic membrane excitability? *2*) Does glycolytic inhibition affect spontaneous neuronal firing? *3*) Does glycolytic inhibition suppress epileptiform network ac-

Fig. 1. Glycolysis, pentose phosphate pathway (PPP), tricarboxylic acid cycle (TCA), and glycolytic inhibition with 2-DG. Diagram shows the main steps in glycolysis, its relationship to the PPP and tricarboxylic acid (TCA) cycle, and the action sites of 2-DG. Briefly, glucose enters cytoplasm via glucose transporters (GLUT3 in neurons or GLUT1 in glia), where glycolysis takes place. Glucose is first phosphorylated to glucose-6-P (G-6-P) and then further catalyzed to pyruvate via multiple steps. Pyruvate is the final product of glycolysis, which then enters mitochondria to participate in the TCA cycle for oxidative ATP production. G-6-P also enters the PPP, which generates reduced nicotinamide adenine dinucleotide phosphate (NADPH) and glutathione (GSH) to prevent the cell damage caused by reactive oxygen species (ROS). When 2-DG is present, it competes with glucose for GLUT3/GLUT1 to enter the cell. Once in the cell, 2-DG is phosphorylated to 2-DG-6-P, which is trapped in the cell and cannot be further metabolized. 2-DG-6-P limits G-6-P conversion to F-6-P, which is the main mechanism of glycolytic inhibition by 2-DG.
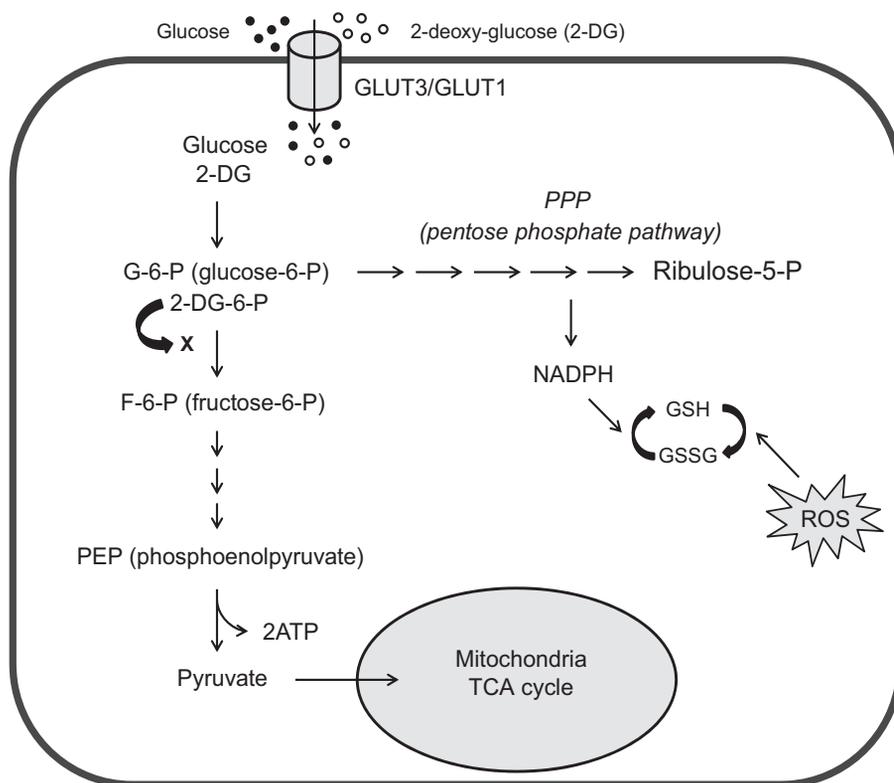
tivity in hippocampal slices from young animals and in a seizure model different from those used in previous studies? and *4*) What is the dose responsiveness and potential toxicity of 2-DG from a cellular perspective?

METHODS

All procedures used in this study were approved by the Institutional Animal Care and Use Committee of Johns Hopkins University.

Brain slice preparation. Experiments were performed in hippocampal slices prepared from 9- to 22-day-old (average: 15 ± 0.7 days, $n = 35$) Sprague-Dawley rats (Harlan, Indianapolis, IN). We chose animals at this age because during this developmental window, the brain (particularly the hippocampal CA3 area) is most susceptible to epileptiform bursting activity in slice electrophysiology experiments (Swann and Brady 1984). After undergoing isoflurane anesthesia, rats were decapitated, and their brains were quickly removed and placed in pre-chilled and oxygenated low-Ca^{2+}/high-Mg^{2+} cutting solution containing (in mM) 125 NaCl, 3 KCl, 1.25 NaH_2PO_4, 25 $NaHCO_3$, 0.25 $CaCl_2$, 10 $MgSO_4$, and 11 glucose for ~2 min. The brain was then evenly dissected into two hemispheres. Brain slices were prepared using a newly designed procedure with a VF-300 compresstome (Precisionary Instruments, Greenville, NC). Briefly, one hemisphere was glued onto the platform of a specimen syringe and embedded with 1.6% low-melting point agarose (type I-B). The specimen syringe with encapsulated tissue block was quickly chilled and transferred into a buffer tank filled with cutting solution. Coronal hippocampal slices (350 μm) were cut and isolated from the embedding agarose, and transferred into a storage chamber filled with a holding solution with lower Ca^{2+} and higher Mg^{2+} concentrations than normal medium (Feldmeyer et al. 2006), containing (in mM) 125 NaCl, 3 KCl, 1.25 NaH_2PO_4, 25 $NaHCO_3$, 0.5 $CaCl_2$, 5 $MgSO_4$, and 11 glucose, and continuously bubbled with 95% O_2 and 5% CO_2. Slices were kept at 34°C for the first 30 min and room temperature thereafter.

Electrophysiology. After 1–2 h of recovery, slices were transferred to a submerged recording chamber and perfused with oxygenated artificial cerebrospinal fluid (aCSF) containing (in mM) 125 NaCl, 3 KCl, 1.25 NaH_2PO_4, 25 $NaHCO_3$, 1.3 $CaCl_2$, 1.3 $MgSO_4$ and 11 glucose. For 0-Mg^{2+} experiments, Mg^{2+} was omitted from aCSF and Ca^{2+} concentration was elevated to 2 mM. All recordings were conducted at 32–33°C through a resistive in-line heater regulated by a low-noise digital temperature control system (Scientifica, East Sussex, UK). Visualization of neurons and manipulation of micropipettes were achieved by a PatchPro 6000 system from Scientifica, which comprises a custom-designed motorized (Z-axis) microscope with infrared-differential interference contrast (IR-DIC) components, light-emitting diode (LED) IR, and fluorescence light sources, a ×40 water-immersion objective and charge-coupled device (CCD) camera, and motorized micromanipulators sitting on a motorized movable base plate, remotely controlled by a control panel and the LinLab software (Scientifica). Electrophysiological recordings were acquired by a MultiClamp 700B amplifier, a Digidata-1550 digitizer, and Clampex 10.4 software (Molecular Devices, Sunnyvale, CA). Single or dual whole cell recordings, extracellular field potential recordings, or simultaneous field potential-whole cell recordings were conducted in hippocampal CA3 or CA1. In some field potential experiments, two slices were recorded simultaneously.

Recording pipettes were pulled from thick-walled [outer diameter (OD) 1.5 mm, inner diameter (ID) 0.86 mm] or thin-walled (OD 1.5 mm, ID 1.1 mm) borosilicate glass with filament through a P-1000 pipette puller (Sutter Instruments, Novato, CA). The electrodes typically have a resistance of 4–8 MΩ. For whole cell and cell-attached recordings, pipettes were filled with internal solution containing (in mM) 130 K-gluconate, 10 HEPES, 5.5 EGTA, 0.5 $CaCl_2$, 1 NaCl, 2 KCl, 1 $MgCl_2$, 10 phosphocreatine-tris, 0.5 Na-GTP, and 2 Mg-ATP; pH was adjusted to 7.25 with 5 M KOH. In some experiments, 2-DG (10 mM) was added to pipette solution to deliver it directly into individual neurons. A 7-mV liquid junction potential between the pipette solution and bath medium was estimated using the junction potential calculator in pCLAMP (Molecular Devices) and was not corrected in the values presented in this article. For field potential recordings, pipettes were filled with aCSF. Whole cell current-clamp

recordings were conducted to examine intrinsic membrane excitability, neuronal firing properties, and network bursting. A series of hyperpolarizing-depolarizing current pulses (500 ms, −200 to +500 pA, step: 50–100 pA) were injected into CA1 pyramidal neurons to determine the input resistance (R_{in}), action potential (AP) threshold, firing pattern, and input-output (I/O) relationship. Field potential recordings (with or without concurrent whole cell recording) were performed in I = 0 mode at high gain ($\alpha = 100$–500). Epileptiform network bursts in CA3 were induced by Mg^{2+}-free medium containing 50 μM 4-AP. 2-DG was bath-applied and diluted from freshly prepared 1 M stock solution for most of the experiments, except those depicted in Figs. 2 and 4A, where 2-DG was applied intracellularly through the recording pipette. All signals were acquired at 10 kHz and low-pass filtered at 2 kHz.

Data analysis. Qualitative and quantitative data analyses were conducted using Clampfit 10.4 (Molecular Devices), SigmaPlot 11 (SPSS, Chicago, IL), and Excel (Microsoft, Redmond, WA) software programs. R_{in} was determined from the peak hyperpolarizing voltage caused by corresponding current injection. Because hyperpolarizing pulses commonly activate H-current (I_h), which causes a "sag-shaped" voltage deflection, the peak voltage level was measured within the first 100 ms of the voltage pulses (i.e., before the sag deflection occurs). AP threshold was defined as the starting point of the first AP

generated by the lowest current injection. The I/O relationship of the neurons was determined by the number of APs generated as the function current injection. The frequencies of spontaneous neuronal firing and network bursting were detected using Clampfit software and presented as events per minute. The dose responsiveness of 2-DG was plotted for efficacy (or toxicity) as the function of 2-DG concentration and fitted with exponential increase (cumulative probability) or exponential decay. One-way ANOVA was used for statistical analysis across multiple groups, followed by the Holm-Sidak test for comparison between each two groups. Student's *t*-test was used for comparisons between two groups. Data are means ± SE, and statistical significance is set to $P < 0.05$.

Pharmacological agents and chemicals. All chemicals used in this study were purchased from Sigma-Aldrich (St. Louis, MO), except 6,7-dinitroquinoxaline-2,3-dione (DNQX; di-sodium salt), which was obtained from Abcam (Cambridge, MA).

RESULTS

Glycolytic inhibition does not alter basal membrane properties of hippocampal pyramidal neurons (CA1). To investigate the consequences of glycolytic inhibition with 2-DG on
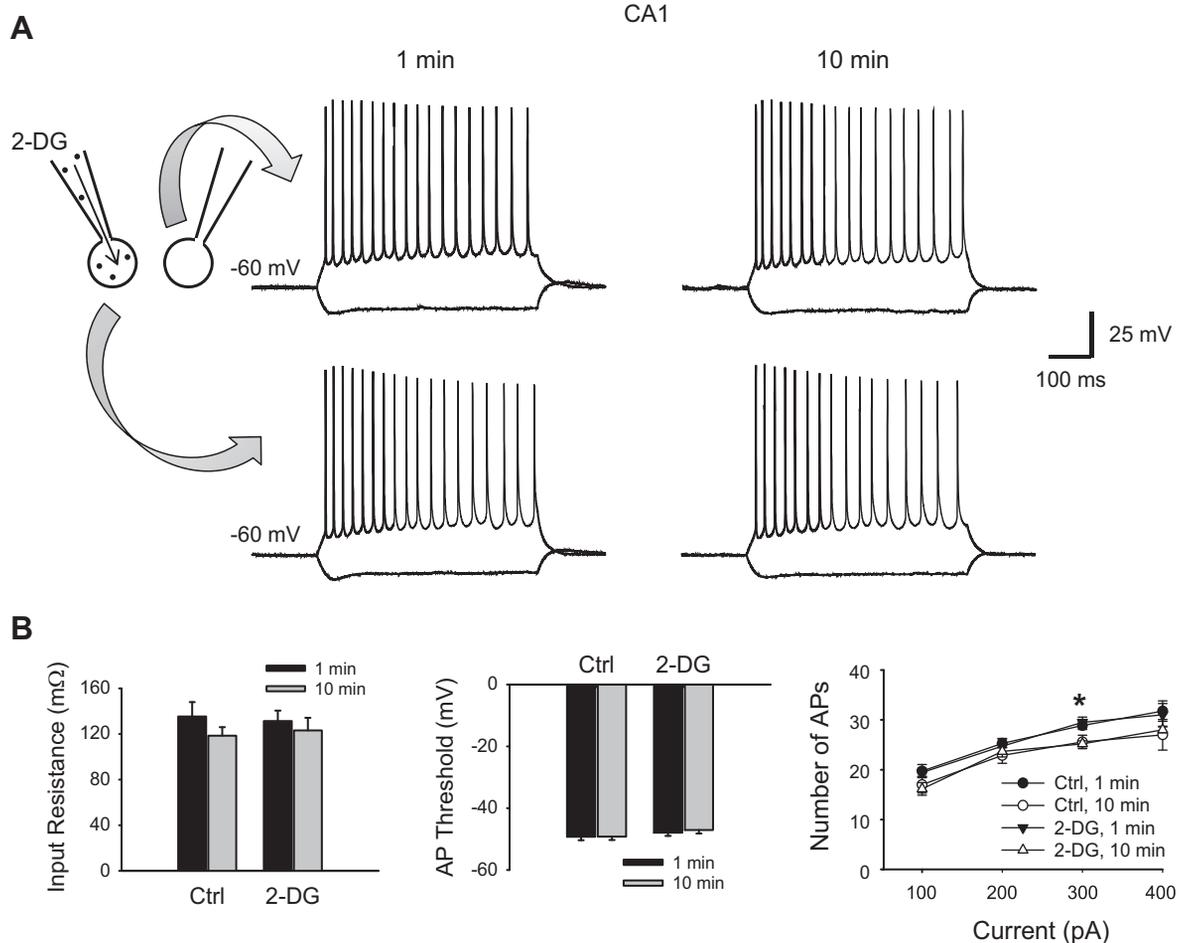

Fig. 2. Glycolytic inhibition with 2-DG does not alter basal membrane excitability of hippocampal CA1 neurons. *A*: two neighboring CA1 pyramidal cells were recorded concurrently, one with 10 mM intracellular 2-DG and one as a control without 2-DG. Their membrane responses to current injection pulses (−200 to +500 pA, 100-pA step, 500 ms) right after rupture of the cell (~1 min) and 10 min after rupture are shown at *left* and *right*, respectively. Note both neurons displayed a regular firing pattern. *B*: summary data showing that the membrane input resistance (*left*) and action potential (AP) threshold (*middle*) were not different between the 2-DG-loaded neurons and controls and did not change over time in the presence of intracellular 2-DG ($P > 0.05$, ANOVA, $n = 7$ pairs). Right, input/output (I/O) relationship (i.e., number of APs as a function of current injection) was also similar between the 2-DG-loaded and control neurons but was slightly reduced after 10 min, particularly at one point in the larger current range (300 pA, *$P < 0.05$). However, both 2-DG-loaded and nonloaded neurons changed in the same direction, and there was no significant difference between them ($P > 0.05$, ANOVA, followed by Holm-Sidak test).

neuronal activity, we first examined whether it alters basal intrinsic membrane properties of neurons. We tested this question in CA1 pyramidal neurons because most CA1 neurons are not spontaneously active (unlike CA3 neurons). Because the uptake of 2-DG is activity dependent (Sokoloff et al. 1977), little 2-DG will be expected to be taken up by these non-active CA1 neurons if applied extracellularly. Therefore, we applied 2-DG (10 mM) intracellularly through the recording pipette. As a control, we simultaneously recorded a neighboring CA1 pyramidal neuron without 2-DG in the pipette solution (Fig. 2A). The intrinsic membrane properties in both neurons were examined immediately after rupture of the membrane (usually within 1 min), and again after 10 min. The resting membrane potentials were similar between the control and 2-DG groups (58 ± 2 vs. 57 ± 1.8 mV, $P > 0.05$, $n = 7$ pairs). Neurons in both groups exhibited a regular firing pattern, which did not alter after 10 min of intracellular 2-DG (Fig. 2A). Similarly, intracellular 2-DG did not significantly alter the input resistance (Fig. 2B, left) or AP threshold (Fig. 2B, middle) after 10-min application (131 ± 9 vs. 123 ± 11 mΩ and 48 ± 1.1 vs. 47 ± 1.1 mV, respectively, $P > 0.05$), which were similar to the values for control neurons (135 ± 13 vs. 119 ± 8 vs. mΩ and 49 ± 1.1 vs. 49 ± 1.1 mV, respectively, $P > 0.05$). The I/O relationship was virtually identical between the control and 2-DG-injected neurons at the beginning of recording and 10 min after (Fig. 2B, right). Notably, the I/O relationship tended to decline slightly with time, particularly in the high current range (e.g., 300 pA, $P < 0.05$). However, both groups changed in the same direction regardless of 2-DG, and there was no difference between the two groups at the same time point and at any given current ($P > 0.05$). These data suggest that glycolytic inhibition with 2-DG does not alter basal intrinsic membrane properties when neurons are in the resting state.

Glycolytic inhibition blocks spontaneous firing of hippocampal pyramidal neurons (CA3) with or without intact synaptic transmission. Next, we examined the effect of glycolytic inhibition with 2-DG on spontaneous firing in active hippocampal neurons (CA3 pyramidal cells). It is known that CA3 neurons are spontaneously active at rest and fire APs in bursts (Hablitz and Johnston 1981; Traub and Wong 1982; Wong and Prince 1978), particularly at young ages (Sipilä et al. 2006). Indeed, under our experimental conditions, most CA3 neurons exhibited robust spontaneous firing in aCSF (Fig. 3). While virtually all recorded CA3 neurons fired in bursts, their spontaneous firing patterns were complex. For example, they might display "clonic-like" firing (i.e., bursts of bursts; Fig. 3A), "tonic-like" firing (continuous-occurring single bursts; Fig. 3B), or mixed clonic and tonic firing, and these patterns were interchangeable over the course of recording. Most bursts were "interictal-like" lasting for a few hundred milliseconds but frequently mixed with "ictal-like" bursts lasting for seconds to tens of seconds (Fig. 3, A and B). Regardless of the firing pattern, bath application of a low concentration of 2-DG (2 mM) completely stopped spontaneous firing after 17.8 ± 2.8 min in 67% of the CA3 neurons ($n = 9$; Fig. 3A). Moreover, the blockade appeared long-lasting in that only partial recovery (low-frequency firing) was observed during washout up to 30 min in these neurons [$n = 4$; but these neurons exhibited no signs of permanent neuronal damage such as the sustained depolarization caused by a higher concentration (10 mM) of 2-DG (see below)]. A higher dose (10 mM) of 2-DG caused sustained

depolarization in active neurons (not shown) and irreversible blockade of network bursts in slices, suggestive of permanent damage (Fig. 5).

CA3 neurons, particularly in immature animals, commonly exhibit robust synaptic activity (Shao and Dudek 2009) due to the extensive recurrent excitatory connections (Miles and Wong 1986), which may contribute to their spontaneous firing. To isolate spontaneous intrinsic bursting from synaptically mediated firing, we pharmacologically blocked both glutamatergic and GABAergic transmission with AMPA-, NMDA-, and GABA$_A$-receptor antagonists DNQX (10 μM), D-aminophosphonovaleric acid (APV; 25 μM), and bicuculline (10 μM), respectively. In the absence of synaptic transmission, CA3 neurons were less active and less prone to fire spontaneously at resting membrane potential. However, when the membrane was modestly depolarized to approximately −55 to 50 mV, the neurons readily and continuously fired robust bursts of APs in a manner similar to that seen with intact synaptic transmission (Fig. 3B). Under these conditions, bath application of 2 mM 2-DG abolished neuronal firing (Fig. 3, B and C) in a similar proportion of neurons (71%, $n = 7$ vs. 67%, $n = 9$ in aCSF; Fig. 3, D and E). Altogether, these data show that glycolytic inhibition results in marked suppression of spontaneous intrinsic bursting.

Blockade of neuronal firing involves glycolytic inhibition of the entire cell population, not just an individual neuron. To test the effect of single-cell glycolytic inhibition on spontaneous firing, we applied 2-DG into individual CA3 neurons through recording pipettes. Surprisingly, although intracellular application of 2-DG (10 mM) reduced the rate of the spontaneous firing in some cells, it failed to stop the spontaneous firing ($n = 6$; Fig. 4, A, C, and D). This finding sharply contrasts with bath application of 2-DG, which completely blocked neuronal bursts (Fig. 4, B and C; see also Fig. 3). These data suggest that when glucose metabolism of an individual neuron is inhibited (i.e., pipette application of 2-DG), it can probably obtain energy/metabolites from extracellular sources to maintain its activity, unless the glucose metabolism of all the cells (neurons and glia) is suppressed (i.e., bath application of 2-DG). Alternatively, the ATP/GTP included in the pipette solution (2.5 mM) may provide some energy for neuronal activity even when glycolysis is inhibited. However, our data showing that bath application of 2-DG effectively blocks spontaneous firing in ATP-loaded neurons argue that the exogenous ATP is probably not enough for intensive and long-lasting neuronal bursting.

Glycolytic inhibition with 2-DG abolishes population bursts in the CA3 neuronal network in a dose-dependent manner. Next, we investigated the effect of glycolytic inhibition on population bursts in the CA3 neuronal networks. To elicit network bursts, we perfused slices with Mg^{2+}-free medium containing 50 μM 4-AP, a well-established model for epileptiform activity (Chen et al. 2014; Kilb et al. 2006; Siniscalchi et al. 1997). We chose this model because pilot experiments showed that the combination of 0-Mg^{2+} and 4-AP-induced field potential population bursts more reliably and faster than other models such as high K$^+$ or 0 Mg^{2+} or 4-AP alone under our experimental conditions, and we also wanted to test the effect of glycolytic inhibition in a seizure model other than those tested in our previous study (Stafstrom et al. 2009).
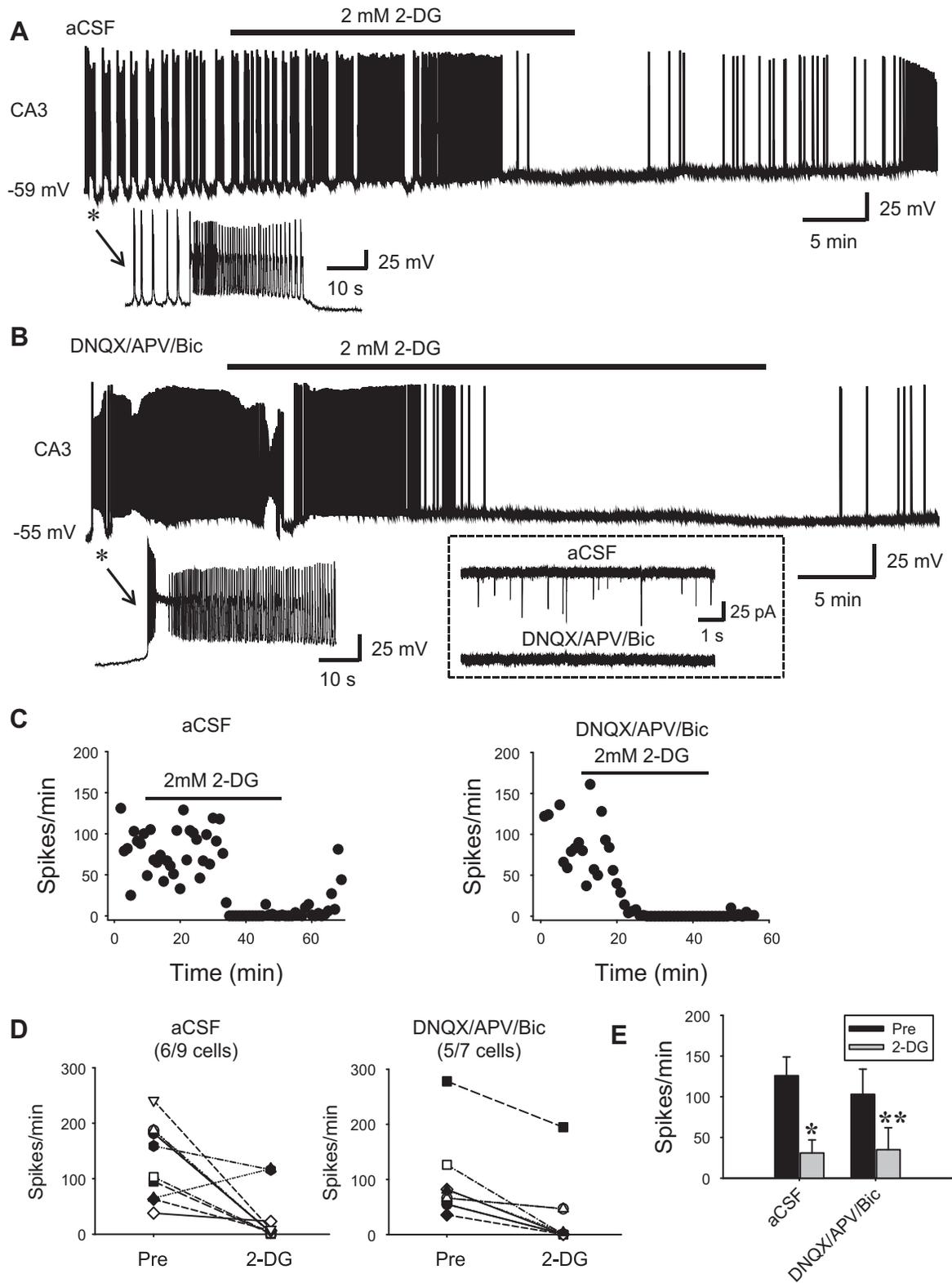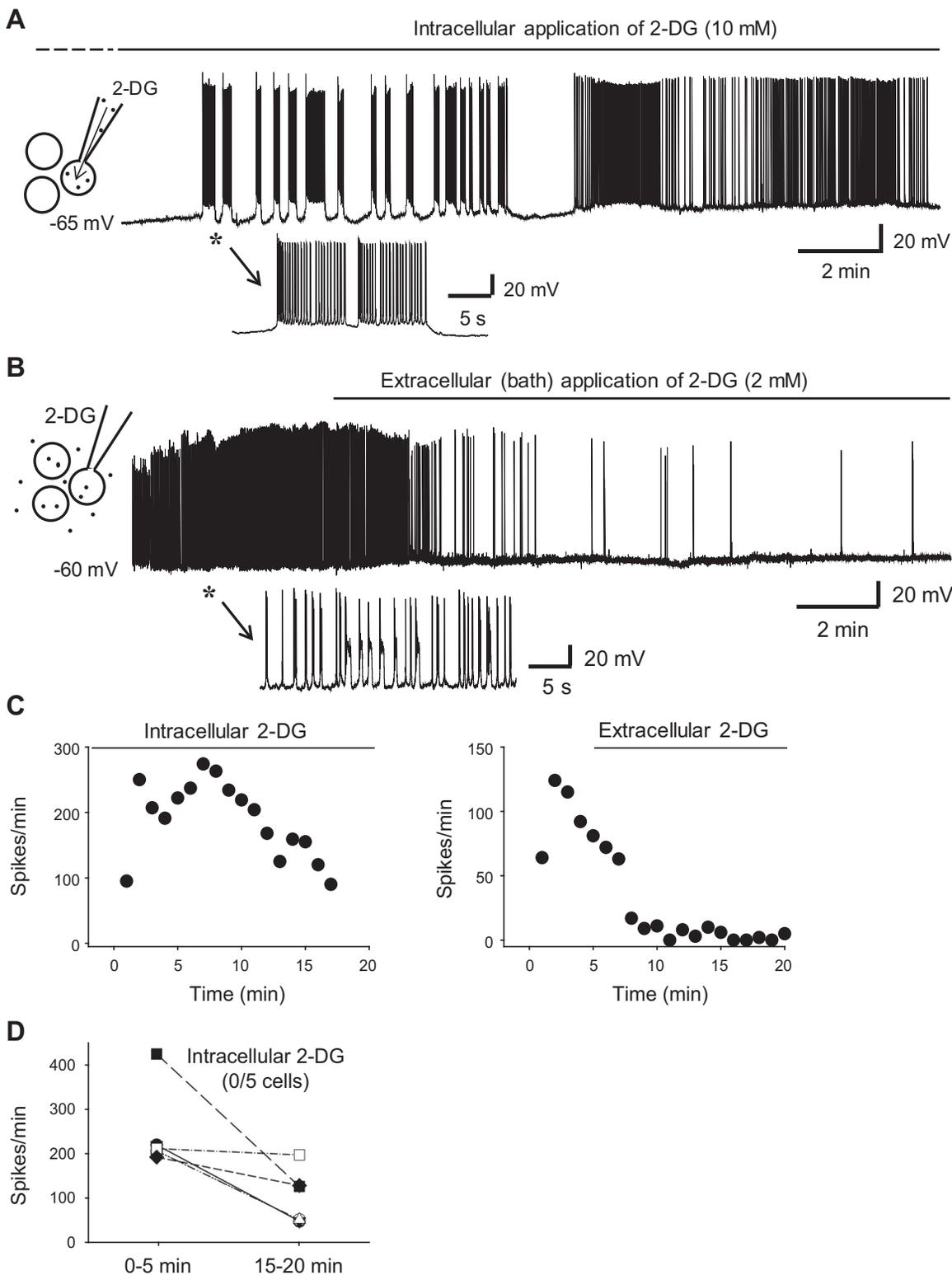
Fig. 3. Glycolytic inhibition abolishes spontaneous firing of the hippocampal CA3 neurons. *A* and *B*: whole cell recordings showing robust spontaneous firing of CA3 pyramidal neurons in aCSF (*A*) or in the presence of synaptic transmission blockers DNQX, APV, and bicuculline (*B*). The asterisks in *A* and *B* mark the initial sections of the recordings, which are expanded (*bottom*) to show the firing patterns of the 2 neurons. *Inset* in dash-lined box in *B* shows that DNQX/APV/Bic completely abolished spontaneous excitatory synaptic currents. Under both conditions, neuronal firing was effectively abolished by bath application of 2 mM 2-DG, which recovered partially during washout. *C*: time course of both the recordings in *A* (*left*) and *B* (*right*) showing the changes in firing rate during 2-DG bath application (horizontal lines). *D*: summary data showing the effect of 2-DG on the individual neurons in the 2 conditions. Note that 2-DG completely blocked spontaneous firing in 6 of 9 and 5 of 7 neurons for the 2 groups, respectively. *E*: averaged firing rate showing the effect of 2-DG in the 2 groups. *$P < 0.05$; **$P < 0.01$, 2-tailed paired *t*-test.

Field epileptiform bursts were consistently induced in the CA3 area minutes after perfusion in 0 Mg^{2+}/4-AP. These bursts are typically "interictal-like," consisting of 1–4 single bursts lasting for 0.1–0.5 s (Fig. 5A). Long-lasting "ictal-like" epileptiform bursts were not common. This pattern of bursting activity is consistent with previous studies (Chen et al. 2014; Kilb et al. 2006; Siniscalchi et al. 1997). Using this model, we tested the efficacy of glycolytic inhibition on network bursting with various doses of 2-DG from 0.5 to 10 mM. As shown in Fig. 5, bath application of low concentration 2-DG (0.5–1 mM) was ineffective in blocking the bursts. At 2 mM, 2-DG completely abolished the population bursts in 54% (7/13) of the slices. The average time to blockade was 14.2 ± 1.6 min. Four of these seven slices exhibited partial recovery during washout

A   Intracellular application of 2-DG (10 mM)

2-DG

-65 mV

*

20 mV

5 s

20 mV

2 min

B   Extracellular (bath) application of 2-DG (2 mM)

2-DG

-60 mV

*

20 mV

5 s

20 mV

2 min

C

Intracellular 2-DG

Extracellular 2-DG

D

Intracellular 2-DG (0/5 cells)

0-5 min   15-20 min

with bursts of much smaller amplitude; three slices showed no washout effect, but two of them displayed frequent single-unit activity (*insets* in Fig. 5A, *middle* trace). These data suggest that 2-DG blockade of network bursts was thorough and long-lasting but does not cause permanent damage to the slices at this concentration (2 mM). At higher concentrations (3.5, 5, and 10 mM), 2-DG blocked population bursts in a progressively higher percentage of slices (78%, 86%, and 95%, respectively; Fig. 5, *C* and *D*) but also led to greater apparent damage to some slices as evidenced by complete and irreversible disappearance of all activity in the slice (both network bursts and single- or multi-unit activity; Fig. 5A, *bottom* trace) or unresponsiveness to electrical stimulation (not shown), particularly at 10 mM. Altogether, these data show that glycolytic inhibition readily abolishes CA3 network bursts in a dose-dependent manner.

Efficacy vs. potential toxicity of glycolytic inhibition on network bursting. We assessed the efficacy of glycolytic inhibition on network burst suppression as the percentage of slices that exhibited full blockade by 2-DG. The potential toxicity was indicated by the decreased "survival" of slices, which is defined as one or more of the following conditions during 2-DG application: *1*) population network bursts persisted (no effect), *2*) network bursts reappeared after washout of 2-DG, and *3*) single- or multi-unit activity was present. Figure 6 summarizes the efficacy and potential toxicity of glycolytic inhibition with 2-DG at various dosages (0.5, 1, 2, 3.5, 5, and 10 mM). With increasing 2-DG concentration, the efficacy of glycolytic inhibition on network burst blockade increases, whereas the survival rate of slices decreases. Notably, 2-DG reaches its steady-state blockade while slice survival dramatically decreases after 3.5 mM (Fig. 6). A dose window of 2–4 mM seems feasible for 2-DG to effectively block network bursting while maintaining viability of most slices. The dose at the intersection of the two curves (~2.7 mM; Fig. 6, vertical dashed line) may be the optimal dose of 2-DG that can theoretically block network bursts while keeping 70% of slices viable (Fig. 6, horizontal dashed line).

DISCUSSION

The main findings of the present study are that *1*) glycolytic inhibition with 2-DG does not directly alter basal intrinsic membrane excitability of nonspontaneously active hippocampal pyramidal neurons (CA1); *2*) glycolytic inhibition with 2-DG effectively blocks spontaneous firing of active hippocampal neurons (CA3); *3*) blockade of neuronal firing involves glycolytic inhibition of the entire cell population and not just a single neuron; and *4*) glycolytic inhibition abolishes

epileptiform network bursts in a dose-dependent manner. Collectively, these data corroborate our previous study that glycolytic inhibition suppresses seizures (Stafstrom et al. 2009) and support multiple other studies demonstrating that cell metabolism plays a central role in neuronal activity (Kawamura et al. 2016; Kim et al. 2015; Lutas and Yellen 2013). More importantly, this study provides detailed cellular-level information about the effects of glycolytic inhibition on neuronal firing and seizure suppression.

Glucose metabolism and neuronal and network excitability. Glucose metabolism provides the main source of energy for normal functioning of the brain and includes two main processes: glycolysis and the tricarboxylic acid cycle (TCA). The former breaks down glucose to pyruvate in the cytosol and produces approximately five to seven ATP molecules; the latter is the common oxidative pathway for both glucose and fatty acids, which further oxidizes pyruvate (via acetyl-CoA) into carbon dioxide and water in mitochondria and produces ~25 ATP molecules (Rich 2003). Although both glucose and fatty acids can be used as fuel sources, brain cells are obligated to use glucose because fatty acids cannot enter brain across the blood-brain barrier. Only under certain conditions (e.g., prolonged fasting or a low-carbohydrate diet) will increased fat metabolism generate ketone bodies that enter the brain to be used as an alternative fuel source. Therefore, under normal conditions, brain tissue depends solely on glucose metabolism for energy production (from both glycolysis and TCA), and thus changes in glucose metabolism may profoundly affect neuronal activity. Our data clearly demonstrate that glycolytic inhibition with 2-DG effectively blocks both neuronal and network bursts, supporting the hypothesis that neuronal and network activity is tightly coupled to glucose metabolism and that an altered metabolic state can profoundly change cellular and network excitability. The blockade of network activity by glycolytic inhibition showed dose dependence (Figs. 5 and 6), with the efficacy of blockade increasing with increasing doses of 2-DG. The dose-dependent blockade of network bursts is unlikely to result from increased osmolality due to the addition of 2-DG (from 0.5 to 10 mM); although hyperosmolality may reduce seizure-like bursting, it takes at least 30 mM glucose to have this effect, and it is easily reversed (Ballyk et al. 1991; Rosen and Andrew 1991), which is not the case here. Rather, 2-DG competes with glucose for transporters and enzymes (Fig. 1). Thus, when the ratio of 2-DG to glucose reaches a critical point (~1:5.5 in our case; i.e., 2 mM 2-DG:11 mM glucose), glycolysis is significantly inhibited. Inhibition of glycolysis decreases the production of

---

Fig. 4. Blockade of neuronal firing requires glycolytic inhibition of the entire cell population, not just a single neuron. *A* and *B*: whole cell recordings of 2 CA3 pyramidal neurons from 2 slices. The recording pipette in *A* contained 10 mM 2-DG to inhibit glycolysis in this neuron, whereas the recording pipette in *B* contained no 2-DG (*inset* diagrams in *A* and *B*). Both neurons were spontaneously active in aCSF. The initial sections of the recordings in *A* and *B* (asterisks) are expanded (*bottom*) to show the firing patterns of the 2 neurons. *A*: the spontaneous firing in this neuron continued when its glycolysis was inhibited with intracellular 2-DG during the entire recording (~25 min). The entire period of intracellular 2-DG exposure (marked by the solid horizontal line above), which started minutes before the recording (i.e., from the rupture of the neuron; dashed line above), was a total of ~30–35 min. Intracellular 2-DG reduced but did not abolish neuronal firing, even at a high concentration (10 mM). *B*: in contrast, glycolytic inhibition of the entire cell population via 2-DG (2 mM) bath application blocked neuronal firing almost completely in just a few minutes. *C*: time course of the recordings in *A* (*left*) and *B* (*right*) showing the changes of neuronal firing rate during 2-DG application (horizontal lines). *D*: summary data showing that none of the recorded neurons (*n* = 5) stopped firing during intracellular 2-DG application (unlike during 2-DG bath application shown in Fig. 3*D*). These data indicate that glycolytic inhibition of a single cell is not sufficient to block its neuronal activity, which may therefore be sustained by some alternative extracellular source of energy/metabolites and is blocked by glycolytic inhibition of the whole cell population (neurons and glia) via bath application of 2-DG.

pyruvate/lactate available to enter TCA, thus greatly reducing ATP production needed to sustain robust epileptiform activity.

Disruption of glycolysis and ATP production may cause broad-spectrum consequences on membrane-bound pumps, channels, and receptors that are important for neuronal activity, particularly the energy-consuming active ion pump Na^+-K^+-ATPase. During epileptiform events, a large amount of Na^+ enters and K^+ exits neurons, which depend on Na^+-K^+-ATPase to restore the transmembrane gradient. Failure of Na^+-K^+-ATPase activity will lead to the collapse of the transmembrane ion gradient, and neuronal firing will eventually cease. In addition, increased intracellular Na^+ will slow
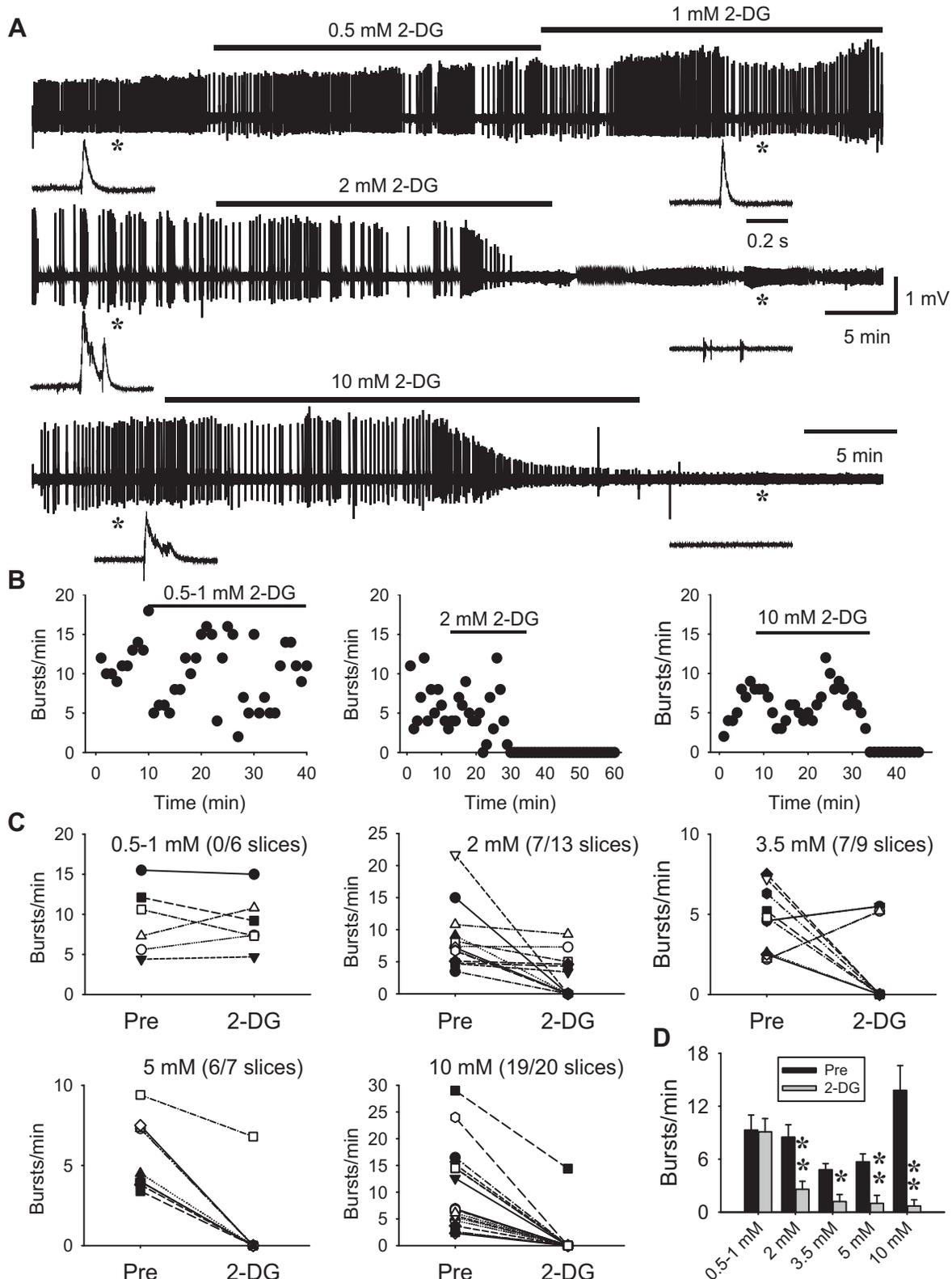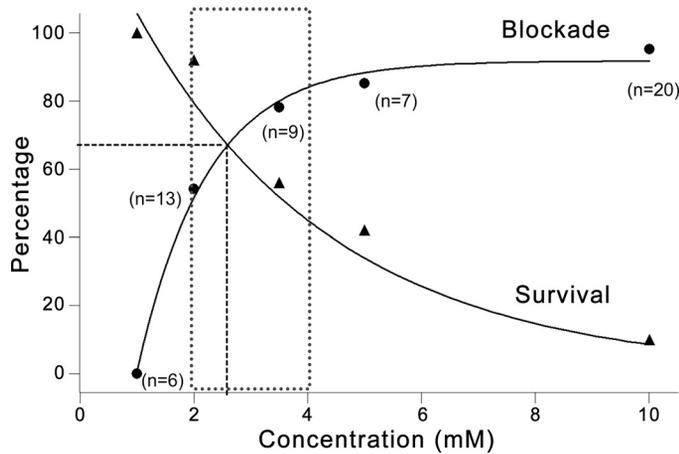
Fig. 6. Dose responses of 2-DG on network burst blockade and slice survival. Graph summarizes the dose responses of 2-DG on network bursts (circles) and on slice survival (triangles), represented by the percentage of slices showing complete burst blockade or the percentage of slice survival (defined in RESULTS) as a function of 2-DG concentration. The blockade curve is fitted with exponential cumulative probability, and the survival curve with exponential decay. In general, burst blockade increases while slice survival decreases with increasing 2-DG concentration. The efficacy of 2-DG burst blockade approaches a steady-state around 3.5 mM, after which slice survival rate drops exponentially. The dotted area represents a feasible dose window for 2-DG (2–4 mM) to effectively block epileptiform bursts while not causing major neuronal damage. The theoretically optimum 2-DG dose may be at the intersection of the two curves, where ~70% slices will stop bursting and remain viable (horizontal dashed line), corresponding to ~2.7 mM 2-DG (vertical dashed line).

Na^+-Ca^{2+} exchange (Török 2007), resulting in an increase of intracellular Ca^{2+}, which in turn activates Ca^{2+}-dependent K^+ channels to hyperpolarize the membrane. Moreover, a reduction of ATP and accumulation of adenosine will activate ATP-sensitive K^+ channels (Ashcroft and Gribble 1998; Lutas and Yellen 2013) and A1 adenosine receptors (Masino and Geiger 2008), leading to membrane hyperpolarization and suppression of seizure activity. Interestingly, neuronal metabolism increases even before seizure onset (Ingram et al. 2014; Wei et al. 2014), suggesting that enhanced energy production is important for seizure initiation. Thus reduced glycolysis can not only block ongoing seizure activity but also may abrogate seizure occurrence.

Another important mechanism by which glycolytic inhibition might block seizures is related to synaptic transmission. It has been proposed that cytosolic ATP produced by glycolysis is important for presynaptic glutamate loading into synaptic vesicles (Ikemoto et al. 2003; Takeda and Ueda 2012). Thus glycolytic inhibition reduces ATP production in the presynaptic terminal, which may decrease glutamate release. A recent preliminary study reported that 2-DG reduces both spontaneous (and miniature) excitatory synaptic currents and spontaneous inhibitory synaptic currents (Pan et al. 2014), supporting this hypothesis. Also, a recent study in hippocampal dentate gyrus neurons showed that 2-DG enhanced tonic GABAergic current and reduced neuron excitability (Forte et al. 2016). In addition, glycolytic inhibition may shift G-6-P into the pentose phosphate pathway (Fig. 1) and increase the production of glutathione, a potential endogenous anticonvulsant (Abe et al. 2000; Lian et al. 2007). These potential mechanisms remain to be investigated in future studies.

It is important to note that neuronal activity depends on ATP not only from neuronal glucose metabolism but likely also from glia. Accumulating evidence has shown that astrocyte-neuron metabolic cooperation is essential for brain energy metabolism, especially during neuronal activity (Bélanger et al. 2011; Magistretti and Pellerin 1996; Nehlig and Coles 2007; Sada et al. 2015). Particularly, glucose taken up by astrocytes also undergoes glycolysis to produce pyruvate, which is converted to lactate, which in turn is shuttled to neurons, where it is converted back to pyruvate and enters the TCA. This pathway is known as "astrocyte-neuron lactate shuttle," which is critical in controlling neuronal activity (Bélanger et al. 2011; Sada et al. 2015) In our study, bath application of 2-DG effectively shuts down neuronal and network activity, likely because 2-DG inhibits glycolysis in both neurons and glia. In contrast, intracellular application of 2-DG inhibits glycolysis only in the recorded neuron but fails to stop its spontaneous firing (Fig. 4), supporting the hypothesis that neurons may obtain fuel supply through the astrocyte-neuron lactate shuttle to maintain their activity.

Potential clinical use of 2-DG as an anti-seizure agent. Accumulating preclinical evidence supports the potential of 2-DG as a clinically useful agent for seizure prevention or treatment. 2-DG reduces seizures in a wide diversity of animal models, supporting a broad mechanism of action that differs from all currently available anti-seizure drugs. For example, 2-DG suppresses seizures elicited by 6-Hz corneal stimulation, kindling of the amygdala and olfactory tract, and audiogenic stimuli (in Frings mice), thus spanning both focal-onset and generalized seizures, but it does not suppress maximum electroshock seizures or pentylenetetrazole-induced seizures (Garriga-Canut et al. 2006; Stafstrom et al. 2009). Furthermore, 2-DG has a favorable safety profile with no significant or long-lasting effects on learning, memory, or general health (Ockuly et al. 2012). 2-DG has been used for decades as a radio-tagged label in positron emission tomography (PET) studies to identify metabolically active brain regions, confirming its safety in humans (Elman et al. 1999). Reversible cardiac toxicity in the form of vacuolar degeneration and endothelial cell hypertrophy were reported at high (supratherapeutic) doses of 2-DG (Minor et al. 2010), but these adverse effects can be

Fig. 5. Glycolytic inhibition abolishes epileptiform network bursts induced by 0 Mg^{2+}/4-AP in a dose-dependent, all-or-none manner. *A*: extracellular field potential recordings showing epileptiform bursting activity in hippocampal CA3 induced by 0-Mg^{2+} medium containing 50 μM 4-AP. These bursts were typically "interictal-like," lasting for 0.1–0.5 s (*insets*). Bath application of low concentrations of 2-DG (0.5–1 mM) had no effect on the bursts (*A, top* trace). At 2 mM, 2-DG effectively blocked all network bursts (*A, middle* trace) while single-unit activity persisted (*inset at right*). At a higher dose (10 mM), 2-DG consistently and completely abolished all the network and single-unit activity, and the slice became silent and nonresponsive (*A, bottom* trace), indicating permanent damage. Asterisks indicate the recording sections before and after 2-DG and are shown on an expanded timescale in *insets*. Note that single-unit activity remained in 2 mM 2-DG but was absent in 10 mM 2-DG. *B*: time course of recordings in *A* showing the different effects of 2-DG at different doses. *C*: summary data showing the 2-DG dose response for each slice. Note that 2-DG blockade of network bursts was largely all-or-none; i.e., 2-DG either had no or a minor effect, or completely blocked bursts. The numbers in parentheses indicate the fraction of slices that expressed complete 2-DG blockade out of all slices in each dose group. *D*: averaged burst rate across slices before (Pre) and after 2-DG at various doses. *P < 0.05; **P < 0.01, 2-tailed paired *t*-test.

monitored and averted by following brain natriuretic peptide levels (Terse et al. 2016). Therefore, 2-DG represents a unique compound with antiseizure and antiepileptic actions. Data regarding 2-DG action at the cellular level, as reported in this article, adds to understanding of the spectrum of usefulness and could guide modifications as clinical development proceeds.

In summary, our findings suggest that neuronal and network activity is tightly coupled to the metabolic state and that the glycolytic inhibitor 2-DG can effectively suppress epileptiform activity, which may hold as a novel treatment for drug-resistant epilepsy.

REFERENCES

Abe K, Nakanishi K, Saito H. The possible role of endogenous glutathione as an anticonvulsant in mice. *Brain Res* 854: 235–238, 2000. doi:10.1016/S0006-8993(99)02269-6.

Ashcroft FM, Gribble FM. Correlating structure and function in ATP-sensitive K^+ channels. *Trends Neurosci* 21: 288–294, 1998. doi:10.1016/S0166-2236(98)01225-9.

Ballyk BA, Quackenbush SJ, Andrew RD. Osmotic effects on the CA1 neuronal population in hippocampal slices with special reference to glucose. *J Neurophysiol* 65: 1055–1066, 1991.

Bélanger M, Allaman I, Magistretti PJ. Brain energy metabolism: focus on astrocyte-neuron metabolic cooperation. *Cell Metab* 14: 724–738, 2011. doi:10.1016/j.cmet.2011.08.016.

Chen R, Okabe A, Sun H, Sharopov S, Hanganu-Opatz IL, Kolbaev SN, Fukuda A, Luhmann HJ, Kilb W. Activation of glycine receptors modulates spontaneous epileptiform activity in the immature rat hippocampus. *J Physiol* 592: 2153–2168, 2014. doi:10.1113/jphysiol.2014.271700.

Conklin HW. Cause and treatment of epilepsy. *J Am Osteopath Assoc* 22: 11–14, 1922.

Elman I, Sokoloff L, Adler CM, Weisenfeld N, Breier A. The effects of pharmacological doses of 2-deoxyglucose on cerebral blood flow in healthy volunteers. *Brain Res* 815: 243–249, 1999. doi:10.1016/S0006-8993(98)01137-8.

Feldmeyer D, Lübke J, Sakmann B. Efficacy and connectivity of intracolumnar pairs of layer 2/3 pyramidal cells in the barrel cortex of juvenile rats. *J Physiol* 575: 583–602, 2006. doi:10.1113/jphysiol.2006.105106.

Forte N, Medrihan L, Cappetti B, Baldelli P, Benfenati F. 2-Deoxy-D-glucose enhances tonic inhibition through the neurosteroid-mediated activation of extrasynaptic GABA$_A$ receptors. *Epilepsia* 57: 1987–2000, 2016. doi:10.1111/epi.13578.

Freeman JM, Vining EP. Ketogenic diet: a time-tested, effective, and safe method for treatment of intractable childhood epilepsy. *Epilepsia* 39: 450–451, 1998. doi:10.1111/j.1528-1157.1998.tb01400.x.

Garriga-Canut M, Schoenike B, Qazi R, Bergendahl K, Daley TJ, Pfender RM, Morrison JF, Ockuly J, Stafstrom C, Sutula T, Roopra A. 2-Deoxy-D-glucose reduces epilepsy progression by NRSF-CtBP-dependent metabolic regulation of chromatin structure. *Nat Neurosci* 9: 1382–1387, 2006. doi:10.1038/nn1791.

Gasior M, Yankura J, Hartman AL, French A, Rogawski MA. Anticonvulsant and proconvulsant actions of 2-deoxy-D-glucose. *Epilepsia* 51: 1385–1394, 2010. doi:10.1111/j.1528-1167.2010.02593.x.

Geyelin HR. Fasting as a method for treating epilepsy. *Med Rec* 99: 1037–1039, 1921.

Hablitz JJ, Johnston D. Endogenous nature of spontaneous bursting in hippocampal pyramidal neurons. *Cell Mol Neurobiol* 1: 325–334, 1981. doi:10.1007/BF00716267.

Hertz L, Dienel GA. Energy metabolism in the brain. *Int Rev Neurobiol* 51: 1–102, 2002. doi:10.1016/S0074-7742(02)51003-5.

Huttenlocher PR. Ketonemia and seizures: metabolic and anticonvulsant effects of two ketogenic diets in childhood epilepsy. *Pediatr Res* 10: 536–540, 1976. doi:10.1203/00006450-197605000-00006.

Ikemoto A, Bole DG, Ueda T. Glycolysis and glutamate accumulation into synaptic vesicles. Role of glyceraldehyde phosphate dehydrogenase and 3-phosphoglycerate kinase. *J Biol Chem* 278: 5929–5940, 2003. doi:10.1074/jbc.M211617200.

Ingram J, Zhang C, Cressman JR, Hazra A, Wei Y, Koo YE, Žiburkus J, Kopelman R, Xu J, Schiff SJ. Oxygen and seizure dynamics: I. Experiments. *J Neurophysiol* 112: 205–212, 2014. doi:10.1152/jn.00540.2013.

Kawamura MJ, Ruskin DN, Masino SA. Metabolic therapy for temporal lobe epilepsy in a dish: investigating mechanisms of ketogenic diet using electrophysiological recordings in hippocampal slices. *Front Mol Neurosci* 9: 112, 2016. doi:10.3389/fnmol.2016.00112.

Kilb W, Dierkes PW, Syková E, Vargová L, Luhmann HJ. Hypoosmolar conditions reduce extracellular volume fraction and enhance epileptiform activity in the CA3 region of the immature rat hippocampus. *J Neurosci Res* 84: 119–129, 2006. doi:10.1002/jnr.20871.

Kim DY, Simeone KA, Simeone TA, Pandya JD, Wilke JC, Ahn Y, Geddes JW, Sullivan PG, Rho JM. Ketone bodies mediate antiseizure effects through mitochondrial permeability transition. *Ann Neurol* 78: 77–87, 2015. doi:10.1002/ana.24424.

Lian XY, Khan FA, Stringer JL. Fructose-1,6-bisphosphate has anticonvulsant activity in models of acute seizures in adult rats. *J Neurosci* 27: 12007–12011, 2007. doi:10.1523/JNEUROSCI.3163-07.2007.

Lutas A, Yellen G. The ketogenic diet: metabolic influences on brain excitability and epilepsy. *Trends Neurosci* 36: 32–40, 2013. doi:10.1016/j.tins.2012.11.005.

Magistretti PJ, Pellerin L. Cellular bases of brain energy metabolism and their relevance to functional brain imaging: evidence for a prominent role of astrocytes. *Cereb Cortex* 6: 50–61, 1996. doi:10.1093/cercor/6.1.50.

Masino SA, Geiger JD. Are purines mediators of the anticonvulsant/neuroprotective effects of ketogenic diets? *Trends Neurosci* 31: 273–278, 2008. doi:10.1016/j.tins.2008.02.009.

Miles R, Wong RK. Excitatory synaptic interactions between CA3 neurones in the guinea-pig hippocampus. *J Physiol* 373: 397–418, 1986. doi:10.1113/jphysiol.1986.sp016055.

Minor RK, Smith DL Jr, Sossong AM, Kaushik S, Poosala S, Spangler EL, Roth GS, Lane M, Allison DB, de Cabo R, Ingram DK, Mattison JA. Chronic ingestion of 2-deoxy-D-glucose induces cardiac vacuolization and increases mortality in rats. *Toxicol Appl Pharmacol* 243: 332–339, 2010. doi:10.1016/j.taap.2009.11.025.

Nehlig A, Coles JA. Cellular pathways of energy metabolism in the brain: is glucose used by neurons or astrocytes? *Glia* 55: 1238–1250, 2007. doi:10.1002/glia.20376.

Ockuly JC, Gielissen JM, Levenick CV, Zeal C, Groble K, Munsey K, Sutula TP, Stafstrom CE. Behavioral, cognitive, and safety profile of 2-deoxy-2-glucose (2DG) in adult rats. *Epilepsy Res* 101: 246–252, 2012. doi:10.1016/j.eplepsyres.2012.04.012.

Pan YZ, Sutula T, Rutecki PA. Evidence for use-dependent and presynaptic actions of 2-DG on abnormal synaptic network activity in the CA3 region of the hippocampus. *Soc Neurosci Abstr* 485: 401, 2014.

Raichle ME, Mintun MA. Brain work and brain imaging. *Annu Rev Neurosci* 29: 449–476, 2006. doi:10.1146/annurev.neuro.29.051605.112819.

Rich PR. The molecular machinery of Keilin's respiratory chain. *Biochem Soc Trans* 31: 1095–1105, 2003. doi:10.1042/bst0311095.

Rosen AS, Andrew RD. Glucose concentration inversely alters neocortical slice excitability through an osmotic effect. *Brain Res* 555: 58–64, 1991. doi:10.1016/0006-8993(91)90859-T.

Sada N, Lee S, Katsu T, Otsuki T, Inoue T. Epilepsy treatment. Targeting LDH enzymes with a stiripentol analog to treat epilepsy. *Science* 347: 1362–1367, 2015. doi:10.1126/science.aaa1299.

Shao LR, Dudek FE. Both synaptic and intrinsic mechanisms underlie the different properties of population bursts in the hippocampal CA3 area of immature versus adult rats. *J Physiol* 587: 5907–5923, 2009. doi:10.1113/jphysiol.2009.179887.

Siniscalchi A, Calabresi P, Mercuri NB, Bernardi G. Epileptiform discharge induced by 4-aminopyridine in magnesium-free medium in neocortical neurons: physiological and pharmacological characterization. *Neuroscience* 81: 189–197, 1997. doi:10.1016/S0306-4522(97)00178-4.

Sipilä ST, Huttu K, Voipio J, Kaila K. Intrinsic bursting of immature CA3 pyramidal neurons and consequent giant depolarizing potentials are driven by a persistent Na^+ current and terminated by a slow Ca^{2+}-activated K^+ current. *Eur J Neurosci* 23: 2330–2338, 2006. doi:10.1111/j.1460-9568.2006.04757.x.

Sokoloff L, Reivich M, Kennedy C, Des Rosiers MH, Patlak CS, Pettigrew KD, Sakurada O, Shinohara M. The [14C]deoxyglucose method for the measurement of local cerebral glucose utilization: theory, procedure, and normal values in the conscious and anesthetized albino rat. *J Neurochem* 28: 897–916, 1977. doi:10.1111/j.1471-4159.1977.tb10649.x.

Stafstrom CE, Ockuly JC, Murphree L, Valley MT, Roopra A, Sutula TP. Anticonvulsant and antiepileptic actions of 2-deoxy-D-glucose in epilepsy models. *Ann Neurol* 65: 435–447, 2009. doi:10.1002/ana.21603.

Stafstrom CE, Rho JM. The ketogenic diet as a treatment paradigm for diverse neurological disorders. *Front Pharmacol* 3: 59, 2012. doi:10.3389/fphar.2012.00059.

Stafstrom CE, Sutula TP. Metabolic control of seizures through inhibition of glycolysis. In: *Ketogenic Diet and Metabolic Therapies*, edited by Masino SA. New York: Oxford University Press, 2017, p. 353–361.

Swann JW, Brady RJ. Penicillin-induced epileptogenesis in immature rat CA3 hippocampal pyramidal cells. *Brain Res* 12: 243–254, 1984. doi:10.1016/0165-3806(84)90046-4.

Takeda K, Ueda T. Enhanced glutamate uptake into synaptic vesicles fueled by vesicle-generated ATP from phosphoenolpyruvate and ADP. Proposed role of a novel enzyme. *Neurochem Res* 37: 2731–2737, 2012. doi:10.1007/s11064-012-0864-4.

Terse PS, Joshi PS, Bordelon NR, Brys AM, Patton KM, Arndt TP, Sutula TP. 2-Deoxy-D-glucose (2-DG)-induced cardiac toxicity in rat: NT-proBNP and BNP As Potential Early Cardiac Safety Biomarkers. *Int J Toxicol* 35: 284–293, 2016. doi:10.1177/1091581815624397.

Thakur KT, Probasco JC, Hocker SE, Roehl K, Henry B, Kossoff EH, Kaplan PW, Geocadin RG, Hartman AL, Venkatesan A, Cervenka MC. Ketogenic diet for adults in super-refractory status epilepticus. *Neurology* 82: 665–670, 2014. doi:10.1212/WNL.0000000000000151.

Török TL. Electrogenic Na^+/Ca^{2+}-exchange of nerve and muscle cells. *Prog Neurobiol* 82: 287–347, 2007. doi:10.1016/j.pneurobio.2007.06.003.

Traub RD, Wong RK. Cellular mechanism of neuronal synchronization in epilepsy. *Science* 216: 745–747, 1982. doi:10.1126/science.7079735.

Wei Y, Ullah G, Ingram J, Schiff SJ. Oxygen and seizure dynamics: II. Computational modeling. *J Neurophysiol* 112: 213–223, 2014. doi:10.1152/jn.00541.2013.

Wong RK, Prince DA. Participation of calcium spikes during intrinsic burst firing in hippocampal neurons. *Brain Res* 159: 385–390, 1978. doi:10.1016/0006-8993(78)90544-9.